International Journal of Energy Research

INTERNATIONAL JOURNAL OF ENERGY RESEARCH
Int. J. Energy Res. 2013; **37**:1562–1568
Published online 17 December 2012 in Wiley Online Library (wileyonlinelibrary.com). DOI: 10.1002/er.2999

TECHNICAL NOTE

A validation study of lithium-ion cell constant c-rate discharge simulation with Battery Design Studio®

Apurba Sakti[1,*,†], Jeremy J. Michalek[1,2], Sang-Eun Chun[3] and Jay F. Whitacre[1,3]

[1]Department of Engineering and Public Policy, Carnegie Mellon University, Pittsburgh, PA 15213
[2]Department of Mechanical Engineering, Carnegie Mellon University, Pittsburgh, PA 15213
[3]Department of Materials Science and Engineering, Carnegie Mellon University, Pittsburgh, PA 15213

SUMMARY

We compare battery performance simulations from a commercial lithium-ion battery modeling software package against manufacturer performance specifications and laboratory tests to assess model validity. A set of commercially manufactured spiral wound lithium-ion cells were electrochemically tested and then disassembled and physically characterized. The Battery Design Studio® (BDS) software was then used to create a mathematical model of each battery, and discharge simulations at constant C-rates ranging from C/5 to 2C were compared against laboratory tests and manufacturer performance specifications. Results indicate that BDS predictions of total energy delivered under our constant C-rate battery discharge tests are within 6.5% of laboratory measurements for a full discharge and within 2.8% when a 60% state of charge window is considered. Average discrepancy is substantially lower. In all cases, the discrepancy in simulated vs. manufacturer specifications or laboratory results of energy and capacity delivered was comparable to the discrepancy between manufacturer specifications and laboratory results. Results suggest that BDS can provide sufficient accuracy in discharge performance simulations for many applications.

KEY WORDS

Battery Design Studio®; lithium-ion; battery performance simulation; constant C-rate discharge; validation

Correspondence

*Apurba Sakti, Department of Engineering and Public Policy.
†E-mail address: asakti@cmu.edu

Received 17 August 2012; Revised 4 November 2012; Accepted 6 November 2012

1. INTRODUCTION

Existing battery modeling and simulation literature includes work on the general energy balance of a battery system [1], the heat generation rate using the energy balance model [2], electrochemical-thermal modeling and experimental validation [3], and the simulation and optimization of lithium-ion battery systems [4] amongst others that involve detailed calculations for the internal electrochemical processes using physics-based models [5–9]. Models that avoid such detail and use approximations to represent a battery system with an equivalent circuit have also been developed and have been shown to match well with manufacturer's data [10] or predict cell performance with accuracy [11]. However, in an equivalent circuit model, where common electrical components like resistors and capacitors are used to represent a battery system, the key elements of battery functionality that are related to ionic diffusion are very difficult to capture since modeling options there involve the use of multiple Warburg diffusion terms. The Battery Design Studio® (BDS) battery simulation software provides versatility by allowing users to select from a set of battery system simulation models (which include both detailed physics based models as well as equivalent circuit ones) and run simulations through a graphical user interface. For this study, the model used is based on the same system of six coupled and non-linear discretized partial differential equations in the full system model described by Fuller *et al.* [4],[1] with time and space as the independent variables. Fuller *et al.* linearized and solved the equations using the BAND solver with the Crank-Nicholson implicit method to evaluate time derivatives [4]. The BAND solver, developed by Newman, uses tridiagonally banded matrices together with the Newton-Raphson method to solve finite difference representations of ordinary differential equations [12]. However, BDS uses a pentadiagonal BAND solver instead and implements more efficient data structures by saving only solid-phase concentrations at each time step. Cell temperature is determined from the overall energy balance calculations using the equations for insertion battery systems developed by Rao and Newman [2].

[1]The Distributed model was also used to simulate the cells at a later stage, and the results were found to be the same.

We aim to assess whether BDS is able to produce battery performance data that can be directly matched to Li-ion cells acquired on the open market. The main motivation behind this work is that a techno-economic optimization of lithium-ion battery packs for different electrified vehicles is currently in progress in which BDS is being used to predict the performance of the battery packs, and this study was intended to ensure that the results from BDS are accurate enough to the extent of our economic modeling. To our knowledge, prior peer-reviewed validation work on BDS exists only for primary lithium-ion coin cells in a study by Yeduvaka *et al*. [13]. Yeduvaka *et al*. discretized discharge curves obtained from manufacturer's data sheets (Sony, Panasonic, Gold Peak, Varta, and Maxell) at different loads and temperatures and adjusted several cell parameters using BDS's built-in parameter estimation (optimization) feature to fit the discretized data. Yeduvaka *et al*. used Gering's AEM approach to estimate the electrolyte properties [14]. With the estimated parameters, Yeduvaka *et al*. reported that the BDS model simulations match the discharge voltage behavior from the manufacturer's data sheet 'fairly well' with greater discrepancies at higher positive electrode thicknesses (3.457 mm, Panasonic CR2354 and 1.8 mm, Sony CR2032) and at temperatures less than −10 °C. Yeduvaka *et al*. do not provide any metric to quantify the accuracy of their comparisons, but examining their data, we find a discrepancy of around 10% between the BDS and the manufacturer's data sheet discharge curves at 23 °C for the Sony CR2032 cell by integrating the area under the curves using the trapezoidal rule. Yeduvaka *et al*. suggested that this discrepancy between the actual and modeled data may be due to a difference in the assumed and actual electrolyte formulation. However, in their study, Yeduvaka *et al*. did not test the cells for their discharge performance in the laboratory. We expand on this prior work by testing vehicle-relevant secondary lithium-ion cells of LiNiCoMn/graphite chemistry with cylindrical form factor in the laboratory and then comparing the results with the manufacturer's data sheet and the BDS simulations. We quantify the accuracy of the discharge curves, keeping in mind vehicle-relevant state-of-charge swings to determine the suitability of BDS for such modeling work.

2. MATERIAL AND METHODS

To test the veracity of BDS, we compare battery discharge performance data (in the format of cell potential vs. discharged capacity at various current loadings) of a set of spirally wound 18650 cells with a $LiNi_{0.33}Mn_{0.33}Co_{0.33}O_2$ cathode active material chemistry and a minimum nominal capacity of 2.05 Ah that were procured from Sanyo. The intended use of these cells, as listed by Sanyo, included electric vehicles [15] and could be implemented in the approach espoused by Tesla Motors Inc., where a large number of 18650 cells are connected in parallel and series to make a large format automotive pack. Data used to inform the comparisons were obtained from three sources: (i) lab tests performed on the cells, (ii) the manufacturer's specification sheet, and (iii) results from the BDS simulations. The co-ordinates of several points on the manufacturer's discharge curve specifications were read and used to approximate the manufacturer's discharge curve. The flow diagram shown in Figure 1 indicates the entire process.

The performance of the Sanyo LiNiCoMn cells was then tested in the laboratory under different C-rate discharges using an Arbin BT2000 test stand. For the sake of comparison, C-rates were chosen based on the discharge curves provided by the manufacturer in their specification sheet. Sample cells were then disassembled in the laboratory, and the following parameters were measured and used as BDS input: electrode thickness and length, active material density, collector thickness, separator length and thickness, jellyroll weight, height and diameter, and cell weight. The exact chemistry of the cathode active material was determined using an X-ray diffractometer (X'Pert Pro MPD for powder samples), and the peaks correspond to those seen for $LiNi_{0.33}Co_{0.33}Mn_{0.33}O_2$ [16] as shown in Figure 2. Electrode structure and morphology in the electrode samples were estimated with the aid of scanning electron microscopy (SEM) (Philips, XL30). Plan-view SEM micrographs, shown in Figure 3, were obtained for the electrode samples and the average particle radius calculated. Table I summarizes the measured and calculated parameters for the cell. The density of $LiNi_{0.33}Co_{0.33}Mn_{0.33}O_2$ was calculated using the lattice dimensions reported by MacNeil *et al*. [17] and was found to be approximately 4.7 g/cm^3. The measured value of the coating density for the cathode, which

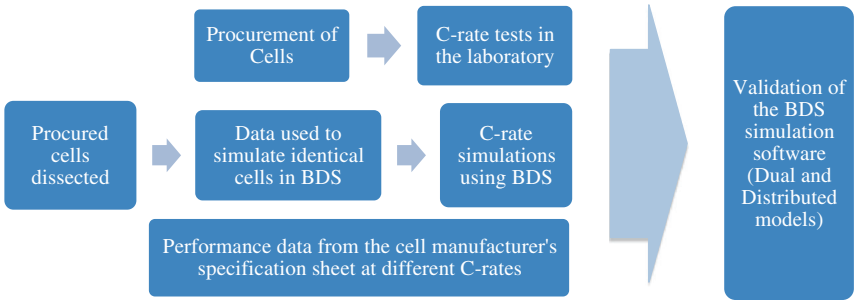

Figure 1. Flow diagram showing the methodology used in the validation study comparing three different data sources to verify Battery Design Studio®. The Dual and Distributed IET (current, potential, and temperature) models were used.

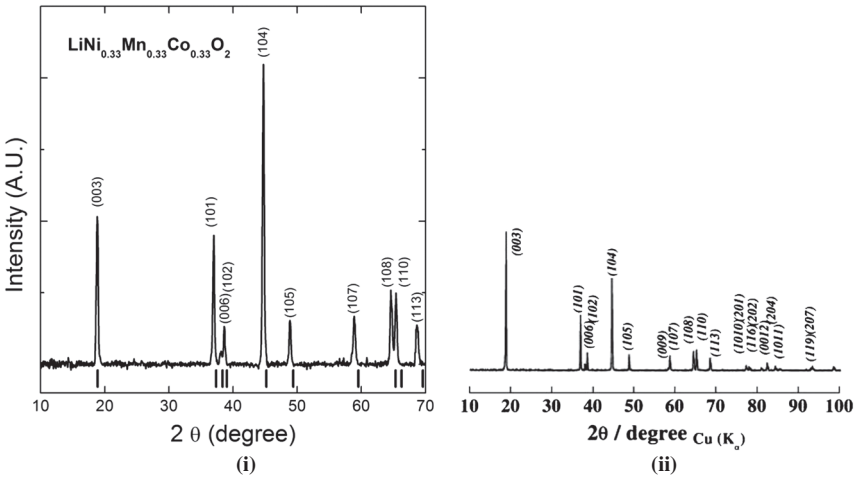

Figure 2. X-ray diffraction data collected from the cathode material has been shown in (i). X-ray diffraction data of $LiNi_{0.33}Co_{0.33}Mn_{0.33}O_2$ adapted from that reported by Yabuuchi and Obzuku [14] has been shown in (ii). The peaks match up indicating that the cathode active material is $LiNi_{0.33}Co_{0.33}Mn_{0.33}O_2$.

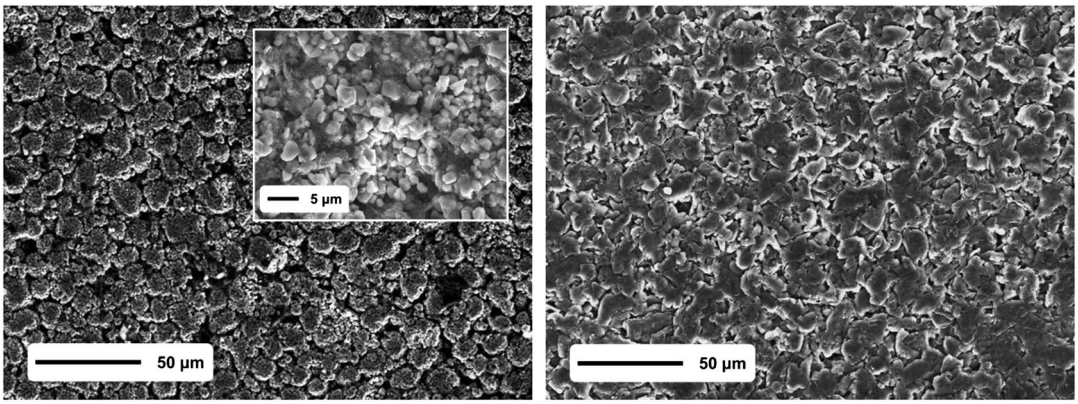

Figure 3. SEM micrographs of the cathode (left) and anode, used to estimate particle size.

Table I. Measured and calculated parameters from the Sanyo LiNiCoMn cell after dissecting them in the laboratory.

Cell		
Weight (g)	42 (+/− 1)	
Jellyroll		
Height (cm)	5.6 (+/− 0.1)	
Length (cm)	78.7 (+/− 0.1)	
Separator		
Length (cm)	162 (+/− 1)	
Thickness (mm)	0.015 ((+/− 0.001)	
Electrodes	Cathode	Anode
Chemistry (cathode from XRD)	$LiNi_{0.33}Co_{0.33}Mn_{0.33}O_2$	graphite
Active material density (g/cm^3)	4.7	-[a]
Single side coat thickness (mm)	0.15 (+/− 0.01)	0.14 (+/− 0.01)
Collector thickness (Al) (mm)	0.014 (+/− 0.001)	0.016 (+/− 0.001)
Coat density (g/cm^3)	3.0 (+/− 0.1)	1.9 (+/− 0.1)
Particle radius from SEM (µm)	0.98 (+/− 0.05)	7.78 (+/− 0.05)

[a]The default density value of 2.25 g/cm^3 was assumed, which was found to be similar to what has been reported elsewhere in the literature [16].

Int. J. Energy Res. 2013; **37**:1562–1568 © 2012 John Wiley & Sons, Ltd.
DOI: 10.1002/er

included the binder and the conductivity aid, was found to be 3.0 g/cm^3. In the case of the anode, a coat density of 1.9 g/cm^3 was measured, and the default graphite density of 2.25 g/cm^3 was assumed, which is similar to what has been reported elsewhere in the literature [18]. Other assumptions made while simulating the cells in BDS are shown in Table II and elaborated in the next section. The simulated cell was then subjected to the same C-rate discharge tests in BDS.

2.1. Assumptions

Wherever possible, the parameters measured from the dissected cells were used as direct inputs in BDS. However, where data were not available, reasonable assumptions were made. This is justifiable because many of the assumed values are common in the industry. For the density of the electrode active material, the mass fractions of the conductive additive and the binder along with the porosity fraction were varied in BDS within their usual ranges to identify plausible combinations that match the density values calculated from dissecting the physical cells in the laboratory. Both density and porosity estimates are consistent with simple analyses performed on the SEM data presented in Figure 3. The electrolyte was assumed to be $LiPF_6$ dissolved in equal weight fractions of ethylene carbonate and ethyl methyl carbonate, a common blend used widely [19]. The separator was assumed to be polypropylene with a porosity of 40%, an average value of porosity of separators available commercially [20]. The equilibrium cell potential curve along with all other parameters including the diffusion coefficient, resistivity, reaction rate constant, theoretical specific capacity, tortuosity, conductivity of the active materials (listed in Table II) were values available in the BDS data base, which is updated frequently. The equilibrium cell potential curves have been shown in Figure 4. The equilibrium cell potential curve of $LiNi_{0.33}Co_{0.33}Mn_{0.33}O_2$ was seen to be in general agreement with what has been reported in the literature for $Li[Ni_xCo_{1-2x}Mn_x]O_2$ $(0 \le x \le 1/2)$ [17]. The theoretical capacity of $LiNi_{0.33}Co_{0.33}Mn_{0.33}O_2$ in the voltage range of 3–4.2 V was found to be around 120 mAh/g which is within the range of 110–130 mAh/g reported by MacNeil *et al.* for $Li[Ni_xCo_{1-2x}Mn_x]O_2$ $(0 \le x \le 1/2)$ [17].

Table II. Assumptions made for different parameters while simulating the cells using BDS.

Electrode parameters	Cathode	Anode
Mass fraction active material	0.84	0.96
Mass fraction binder (ethylene-propylene copolymer)	0.03	0.015
Mass fraction of conductive aid (graphite)	0.13	0.025
Porosity fraction	0.195	0.17
Active material diffusion coefficient (solid) (cm^2/s at 25 °C)	3E-11	6.74E-11
Active material lithium site concentration before formation (used to calculate the stoichiometry) (mAh/g)	275	370
Resistivity (Ωm^2 at 25 °C)	6E-3	0.5
Reaction rate constant (mA/cm^2)	1.08E2	2.02E-01
Electrode conductivity (S/cm)	100	100
Tortuosity (Bruggemann Exp)	1.25	1.9
Other Parameters		
Initial salt concentration, $LiPF_6$ in EC:EMC (M)	1.0	
Electrolyte density (g/cm^3)	1.25	
Separator material (polypropylene) density (g/cm^3)	0.65	
Aluminum density (g/cm^3)	2.7	
Copper density (g/cm^3)	8.9	

3. RESULTS AND DISCUSSION

The comparison of the constant current discharge profiles for the cell is shown in Figure 5. The results from the laboratory match closely with the results from the manufacturer's specification sheet, and the results from the BDS simulations predict somewhat higher voltage over most of the range, particularly when mostly discharged. Tables III and IV summarize the difference between delivered energy and delivered capacity measured using BDS, laboratory tests,

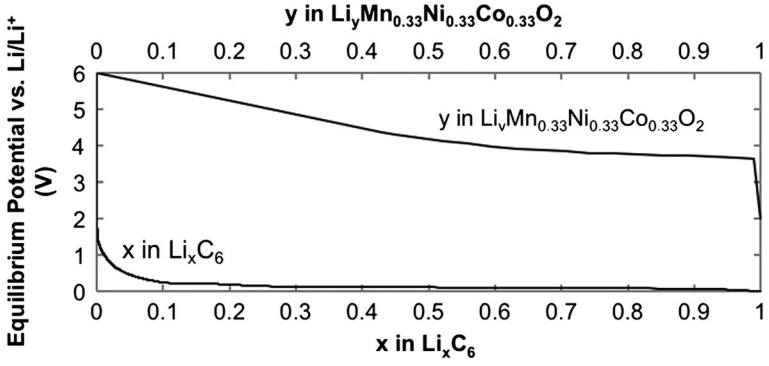

Figure 4. Equilibrium potential curves used in Battery Design Studio® for the $LiNi_{0.33}Co_{0.33}Mn_{0.33}O_2/Li_xC_6$ system.

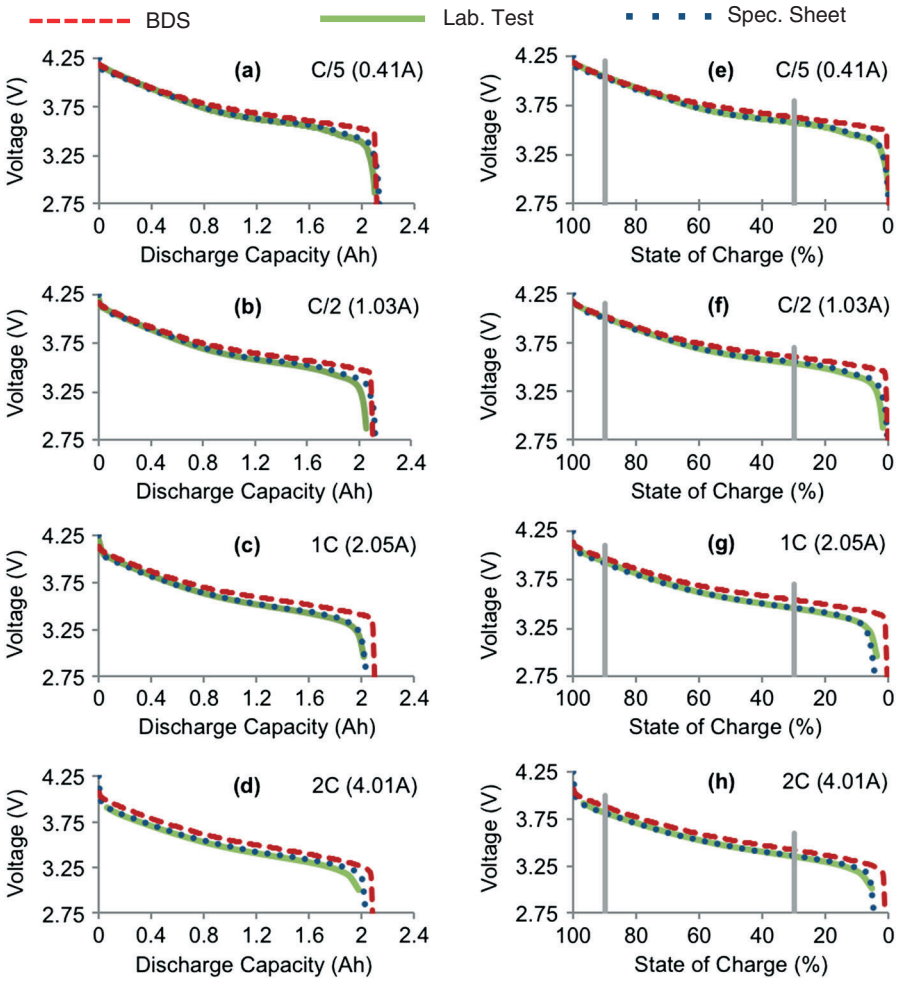

Figure 5. (a–d) shows the comparison of the discharge curves at different C-rate discharges for Sanyo LiNiCoMn cells, while (e–h) show the same discharge curves plotted with respect to their state-of-charge (SoC). The 60% SoC window considered in the study has been shown with two vertical lines. The discharge C-rates and the corresponding currents have been specified for each. The discharge rates were selected based on information in the manufacturer's data sheets to facilitate the comparison.

and the manufacturer specification sheet. Delivered energy in the case of the manufacturer's specification sheet was computed by calculating the area under each of the curves using the trapezoidal rule by selecting points at most 0.1 Ah apart. In the case of the BDS simulations, reporting parameters of 10 s and 0.1 V were selected, leading to results with a resolution within 0.01 Ah.[2] Laboratory results using the Arbin BT2000 test stand reported values using a much higher resolution. The cell simulations predicted capacity and energy within 4.3% of manufacturer specification and within 6.5% of lab tests (Table III). Average discrepancies for the cell simulations are substantially lower.

The discharge profiles were also compared under a reduced 60% state of charge (SoC) window. This was done to simulate similar conditions encountered in some battery applications, such as vehicle applications (e.g. the Chevy Volt battery pack operates within a 65% SoC window [21]). In this case, the magnitude of this SoC swing (in Ah) was calculated based on the measured or modeled total capacity value for each case (Figure 5). The curves were then compared between the 30% and 90% SoC window for the energy and capacity delivered. BDS results match more closely within the 60% SoC. The cell simulations predicted energy and capacity values within 1.6% of manufacturer specification and within 2.8% of lab tests (Table IV). Again, average discrepancies for the cell simulations are substantially lower. The average and maximum difference in the voltage between the discharge curves from the manufacturer's specification sheet and the laboratory results vs. the BDS simulation results within this SoC window were also calculated (Table IV). The maximum difference is within 0.08 V of manufacturer specification and 0.09 V of lab results. Average voltage discrepancies are lower.

[2]Simulations with a tighter resolution of 0.5 s produced similar energy and capacity results within 0.2%, and tests with a more coarse resolution of 1 min produced results within 0.1%.

Int. J. Energy Res. 2013; **37**:1562–1568 © 2012 John Wiley & Sons, Ltd.
DOI: 10.1002/er

Table III. The total delivered energy (Wh), calculated by integrating the discharge curve, along with the capacity (Ah) values as shown in Figure 5. The percent difference of the values with respect to the BDS simulation results has been indicated in parenthesis.

	BDS simulation results		Manufacturer's specification sheet		Laboratory results	
Discharge rate (Current)	Capacity (Ah)	Energy (Wh)	Capacity (Ah)	Energy (Wh)	Capacity (Ah)	Energy (Wh)
C/5 (0.41A)	2.11	7.89	2.13 (0.9)	7.89 (0.0)	2.09 (−0.9)	7.75 (−1.8)
C/2 (1.03A)	2.10	7.81	2.13 (1.4)	7.80 (−0.1)	2.05 (−2.4)	7.53 (−3.6)
1C (2.05A)	2.09	7.68	2.04 (−2.4)	7.35 (−4.3)	2.02 (−3.3)	7.26 (−5.5)
2C (4.1A)	2.08	7.41	2.03 (−2.4)	7.13 (−3.8)	1.98 (−4.8)	6.93 (−6.5)

Table IV. The total delivered energy (Wh), calculated by integrating the discharge curve, along with the capacity (Ah) values for a 60% state of charge window as shown in Figure 5. The percent difference of the values with respect to the BDS simulation results is indicated in parenthesis. The average difference in voltage within the state-of-charge (SoC) window has also been listed along with the maximum voltage difference in parenthesis.

	BDS simulation results		Manufacturer's specification sheet			Laboratory results		
Discharge rate (Current)	Capacity (Ah)	Energy (Wh)	Capacity (Ah)	Energy (Wh)	Avg. (Max) V diff. (V)	Capacity (Ah)	Energy (Wh)	Avg. (Max) V diff. (V)
C/5 (0.41A)	1.26	4.79	1.28	4.80	−0.03	1.26	4.72	−0.04
			(1.6)	(0.2)	(−0.05)	(0.0)	(−1.5)	(−0.05)
C/2 (1.03A)	1.26	4.75	1.28	4.76	−0.03	1.26	4.66	−0.05
			(1.6)	(0.2)	(−0.05)	(0.0)	(−1.9)	(−0.07)
1C (2.05A)	1.26	4.69	1.28	4.66	−0.06	1.26	4.58	−0.06
			(1.6)	(−0.6)	(−0.08)	(0.0)	(−2.3)	(−0.09)
2C (4.1A)	1.26	4.57	1.28	4.54	−0.07	1.26	4.44	−0.09
			(1.6)	(−0.7)	(−0.07)	(0.0)	(−2.8)	(−0.08)

4. CONCLUSION

The energy and capacity calculated from constant C-rate discharge curves simulated using BDS for the Sanyo LiNiCoMn cells were found to be within 6.5% and 4.8% of laboratory data for a full discharge, respectively, and within 2.8% and an exact match of laboratory data for a 60% SoC window, respectively. Average discrepancies are substantially lower and are comparable to discrepancies between laboratory tests and manufacturer specifications. Results indicate that relatively accurate performance predictions are possible using BDS if appropriate parameters are used. Furthermore, by showing agreement between actual data and modeled performance through a range of discharge currents, we provide evidence that this model is able to accurately represent key elements of battery functionality that are related to ionic diffusion through the system.

5. LIMITATIONS

We examine only constant C-rate discharge at room temperature and do not explicitly test charging, variable rate discharge, or elevated temperature. Due to the unavailability of higher C-rate discharge performance from the manufacturer, the C-rates chosen for the discharges were also lower than what is likely to be encountered in electrified vehicle applications. We also use assumed default values for several unknown cell parameters, such as the diffusion coefficient, resistivity, reaction rate constant, tortuosity, and conductivity of the active materials. Model fit might be expected to improve if precise measurements of these parameters were used.

ACKNOWLEDGEMENTS

The authors wish to thank Robert Spotnitz and Gowri Yeduvaka of Battery Design LLC for their valuable guidance during the course of this study. The authors would also like to thank Aquion Energy for use of laboratory facilities. This research was supported in part by support from Gordon and Betty Moore Foundation, a grant from the National Science Foundation, CAREER grant # 0747911, and a grant from Toyota Motor Corporation. The findings and views expressed are those of the authors and not necessarily those of the sponsors.

REFERENCES

1. Bernardi D, Pawlikowski E, Newman J. A general energy balance for battery systems. *Journal of the Electrochemical Society* 1985; **132**:5–12.
2. Rao L, Newman J. Heat-generation rate and general energy balance for insertion battery systems. *Journal of the Electrochemical Society* 1997; **144**:2697–04.
3. Fang W, Kwon OJ, Wang C-Y. Electrochemical-thermal modeling of automotive Li-ion batteries and

experimental validation using a three-electrode cell. *International Journal of Energy Research* 2010; **34**:107–12.
4. Fuller TF, Doyle M, Newman J. Simulation and optimization of the dual lithium ion insertion cell. *Journal of the Electrochemical Society* 1994; **141**:1–10.
5. Doyle M, Fuller TF, Newman J. Modeling of galvanostatic charge and discharge of the lithium/polymer/insertion cell. *Journal of the Electrochemical Society* 1993; **140**:1526–33.
6. Doyle M, Newman J, Gozdz AS, Schmutz CN, Tarascon J. Comparison of modeling predictions with experimental data from plastic lithium ion cells. *Journal of the Electrochemical Society* 1996; **143**:1890–03.
7. Arora P, Doyle M, White RE. Mathematical modeling of the lithium deposition overcharge reaction in lithium-ion batteries using carbon-based negative electrodes. *Journal of the Electrochemical Society* 1999; **146**:3543–53.
8. Song L, Evans JW. Electrochemical-thermal model of lithium polymer batteries. *Journal of the Electrochemical Society* 2000; **147**:2086–95.
9. Gu WB, Wang CY. Thermal-electrochemical modeling of battery systems. *Journal of the Electrochemical Society* 2000; **147**:2910–22.
10. Gao L, Shengyi L, Dougal RA. Dynamic lithium-ion battery model for system simulation. *IEEE Transactions on Components and Packaging Technology* 2002; **25**:495–05.
11. Dubarry M, Vuillaume N, Liaw BY. Origins and accommodation of cell variations in Li-ion battery pack modeling. *International Journal of Energy Research* 2010; **34**:216–31.
12. Spotnitz RM. NL3BO, A framework for electrochemical systems. *Electrochemical Society Proceedings* 1999; **99**(14):242–9.
13. Yeduvaka GS, Spotnitz RM, Gering KL. Macrohomogenous modeling of commercial. Primary Li/MnO_2 coin cells. *Electrochemical Society Transactions* 2009; **19**(16):1–10.
14. Gering KL. Prediction of electrolyte viscosity for aqueous and non-aqueous systems: Results from a molecular model based on ion solvation and a chemical physics framework. *Electrochemica Acta* 2006; **51**:3125–38.
15. Standard Electric Company [Internet]. Japan. Sanyo lithium ion rechargeable batteries; [updated 2009, cited 2012 Jul 18] Available from: http://www.stnd.co.jp/aspx/Class/Class2_2ELithiumIon.2009_E.PDF
16. Yabuuchi N, Ohzuku T. Novel lithium insertion material of $LiCo_{1/3}Ni_{1/3}Mn_{1/3}O_2$ for advanced lithium-ion batteries. *Journal of Power Sources* 2003; **119-121**:171–74.
17. Macneil DD, Lu Z, Dahn JR. Structure and Electrochemistry of $Li[Ni_xCo_{1-2x}Mn_x]O_2$ $(0 \leq x \leq 1/2)$. *Journal of the Electrochemical Society* 2002; **149**: A1332–36.
18. Robertson J. Properties of diamond-like carbon. *Surface and Coatings Technology* 1992; **50**(3):185–03.
19. Ehlrich GM. Lithium-ion batteries. In *Handbook of Batteries*, Linden D, Reddy TB (eds). McGraw-Hill: New York; 2002; 35.22.
20. Ehlrich GM. Lithium-ion batteries. In *Handbook of Batteries*, Linden D, Reddy TB (eds.). McGraw-Hill: New York, 2002; 35.29.
21. General Motors [Internet]. USA. Volt introduces revolutionary Voltec system; [updated 2011 Sept 12; cited 2012 Jul 18]. Available from: http://media.gm.com/content/media/us/en/gm/news.detail.html/content/Pages/news/au/en/2011/Dec/1209_VoltIntroducesRevolutionaryVoltecSystem.html